Int. J. Anal. Appl. (2026), 24:261

International Journal of Analysis and Applications

The Cauchy–Dirichlet Problem for n-Dimensional Hyperbolic Equations with a p-th Degree Trigonometric Source

Zafar Duman Abbasov[1], **Youssri Hassan Youssri**[2], **Manoj Gupta**[3], **Pannee Suanpang**[4], **Aziz Nanthaamornphong**[5,*]

[1]*Department of Mathematical Analysis, Ganja State University, Ganja AZ2000, Azerbaijan*
[2]*Department of Mathematics, Faculty of Science, Cairo University, Giza 12613, Egypt*
[3]*Department of Electrical Engineering, SoS-Engineering & Technology, Guru Ghasidas Vishwavidyalaya (A Central University), Bilaspur (Chhattisgarh), India*
[4]*Department of Information Technology, Faculty of Science and Technology, Suan Dusit University, Bangkok, Thailand*
[5]*College of Computing, Prince of Songkla University, Phuket, Thailand*

[*]*Corresponding author:* aziz.n@phuket.psu.ac.th

Abstract. This paper investigates the Cauchy–Dirichlet problem for a class of n-dimensional non-homogeneous hyperbolic equations characterized by a complex source term. The governing equation incorporates first-order derivatives with respect to both time and spatial coordinates, representing systems with internal dissipation (energy loss) and convection. The non-homogeneous part of the equation is given as a p-th degree power of a multi-harmonic trigonometric sum, which indicates that the temporal dynamics of the system are significantly complex. Since the considered mixed problem is in an n-dimensional setting, we establish the existence and uniqueness of the generalized solution within the framework of Sobolev spaces, specifically $H_0^1(\Omega)$. The convergence of the obtained Fourier series is rigorously proved in the energy norm, ensuring the stability of the analytical solution found for n-dimensional domains. Using the method of eigenfunction expansion (separation of variables) in n-dimensional rectangular domains, a complete analytical and exact solution has been found. Here, the source term is determined by applying the Binomial Theorem, which allows for an explicit representation of the modal forcing coefficients. The temporal variation of each spatial mode is determined via Duhamel's principle, and a bounded solution is obtained that accounts for both the initial conditions and external multi-harmonic excitations.

Received: Jul. 4, 2026.

2020 *Mathematics Subject Classification.* 35L20; 35L05; 35C05; 35C10.

Key words and phrases. n-dimensional hyperbolic equation; Cauchy–Dirichlet problem; analytical solution; binomial expansion; multi-harmonic source; eigenfunction expansion.

https://doi.org/10.28924/2291-8639-24-2026-261
ISSN: 2291-8639

1. Introduction

Hyperbolic partial differential equations form a fundamental area of mathematical physics. They model many physical processes, such as wave propagation, vibrations, and electromagnetic fields. Multi-dimensional hyperbolic systems are especially important for describing complex phenomena in higher dimensions, which appear frequently in acoustics, elasticity, and quantum mechanics.

A key challenge in studying these systems is handling non-homogeneous source terms. While linear sources are well understood, forcing functions given as nonlinear or power series create new analytical difficulties. When the natural frequencies of a bounded n-dimensional domain interact with an external force expressed as the p-th power of a high-order trigonometric Fourier series, complex resonance and instability can arise. This makes it important to study systems subject to periodic but non-harmonic influences, where energy spreads across multiple frequency bands.

In this paper, we study the Cauchy–Dirichlet problem for an n-dimensional hyperbolic equation with a p-th degree trigonometric source term. The equation includes first-order temporal damping and spatial gradient terms, providing a general framework for wave systems. Our main goal is to find an accurate analytical solution by combining eigenfunction expansion with the Binomial Theorem.

We define the solution in the sense of generalized functions to ensure mathematical rigor. Because the problem is multi-dimensional and the source involves high-order harmonics, we use energy methods and Sobolev space theory to study solution regularity. This approach lets us prove uniqueness and stability without requiring very smooth initial data-a common restriction in classical treatments. Recent studies on multidimensional heat transfer and diffusion processes have significantly advanced numerical modeling techniques [1–3].

Our work builds on both classical and modern sources in mathematical physics and PDEs. We rely on foundational texts by Koshlyakov [4], Tikhonov and Samarskii [5], and Sobolev [6]. For Sobolev spaces and generalized solutions, we draw on Ladyzhenskaya [7] and Mikhailov [8]. For global solutions of nonlinear hyperbolic equations, we follow Sattinger [9]. We also use recent teaching and methodological works by Abbasov [10,11], and for boundary function determination in second-order hyperbolic problems, we incorporate results by Askerov [12]. Together, these sources connect classical theory with modern analytical tools.

Spectral methods offer an effective way to approximate differential equations numerically. They use global polynomial bases to achieve fast convergence for smooth solutions [13, 14]. Core ideas-approximation theory, stability, and boundary treatment-are well explained in standard references [13, 14], and recent work extends these methods to problems with varying coefficients and integral terms [15].

Building operational matrices for derivatives is key to efficient spectral discretizations, especially with bases like Bernoulli or shifted Chebyshev polynomials. Recent studies have improved

Galerkin and collocation schemes using Bernoulli polynomials for higher-order and integro-differential equations [16, 17]. Similarly, enhanced operational matrices for shifted Chebyshev bases help solve even-order boundary value problems and fractional derivatives accurately [18–20]. These approaches keep matrix structures sparse and support tensor-product extensions for multi-dimensional problems.

Collocation at Chebyshev–Gauss–Lobatto nodes combines pointwise residual enforcement with spectral accuracy, making it suitable for nonlinear and time-fractional PDEs [21]. For hyperbolic and convection-dominated problems, shifted Jacobi and Chebyshev spectral-Galerkin methods show strong stability and high-order convergence [22]. These results support the combined use of basis selection, operational calculus, and collocation found in modern spectral literature [13, 14]. We consider the mixed boundary value problem for the n-dimensional wave equation. The generalized well-posed solution satisfying non-homogeneous Neumann boundary conditions is studied in Sobolev spaces, and new results are obtained [23].

The paper is organized as follows: Section 2 states the problem and constructs the homogeneous solution. Section 3 analyzes the non-homogeneous source and derives the particular solution. Section 4 presents the full solution and computes the Fourier coefficients. Section 5 proves validity and convergence through lemmas and theorems. Section 6 discusses the physical and mathematical implications. Section 7 introduces the Bernoulli–Chebyshev spectral collocation method. Finally, Section 9 summarizes the main findings.

2. Problem Statement and Homogeneous Solution

2.1. **The Governing Equation and Boundary Conditions.**

The process is described by the following n-dimensional partial differential equation (PDE):

$$u_{tt} + 2\beta u_t - a^2 \Delta u + \sum_{i=1}^{n} b_i u_{x_i} = f(\mathbf{x}, t), \quad \mathbf{x} \in \Omega \subset \mathbb{R}^n, \quad t > 0, \tag{2.1}$$

where $\mathbf{x} = (x_1, x_2, \ldots, x_n)$ and $\Omega = \prod_{i=1}^{n}(0, l_i)$. The parameters $\beta > 0$ and $a > 0$ are constant coefficients. Here, Δ denotes the Laplace operator, and $\sum_{i=1}^{n} b_i u_{x_i}$ represents the first-order spatial derivatives (convection terms).

The non-homogeneous source term $f(\mathbf{x}, t)$ is defined by a power-sum of harmonic oscillations:

$$f(\mathbf{x}, t) = \left[\sum_{k=1}^{m} A_k \cos(\omega_k t + \phi_k)\right]^p. \tag{2.2}$$

We assume that the system is subject to the homogeneous Dirichlet boundary condition on the boundary $\partial\Omega$ of the domain Ω:

$$u(\mathbf{x}, t)\big|_{\partial\Omega} = 0, \quad t \geq 0. \tag{2.3}$$

This physical constraint signifies that the potential (or displacement) u remains zero at the boundaries of the spatial domain. To define the state of the system at the initial time $t = 0$, the following conditions are prescribed:

$$u(\mathbf{x},0) = \Phi(\mathbf{x}), \tag{2.4}$$

$$u_t(\mathbf{x},0) = \Psi(\mathbf{x}), \tag{2.5}$$

where Φ and Ψ are given continuous functions in Ω.

2.2. **Construction of the Homogeneous Solution.** To determine the homogeneous part of the solution, we consider the governing equation (2.1) without the external forcing term ($f \equiv 0$):

$$u_{tt} + 2\beta u_t - a^2\Delta u + \sum_{i=1}^{n} b_i u_{x_i} = 0. \tag{2.6}$$

We assume that the solution u_h can be factored into a product of a spatial function $X(\mathbf{x})$ and a temporal function $T(t)$:

$$u_h(\mathbf{x},t) = X(\mathbf{x})T(t). \tag{2.7}$$

By substituting (2.7) into (2.6), we obtain:

$$XT'' + 2\beta XT' - a^2 T\Delta X + T\sum_{i=1}^{n} b_i X_{x_i} = 0.$$

Dividing the entire equation by XT and rearranging the terms to isolate the variables, we get:

$$\frac{T'' + 2\beta T'}{a^2 T} = \frac{\Delta X - \frac{1}{a^2}\sum_{i=1}^{n} b_i X_{x_i}}{X} = -\lambda,$$

where λ is the separation constant. This equality leads to two independent ordinary differential equations (ODEs). The spatial part of the equation yields:

$$\Delta X - \frac{1}{a^2}\sum_{i=1}^{n} b_i X_{x_i} + \lambda X = 0, \tag{2.8}$$

subject to the homogeneous Dirichlet boundary condition:

$$X(\mathbf{x})\big|_{\partial\Omega} = 0. \tag{2.9}$$

Solving this boundary value problem for a given domain Ω provides a discrete set of eigenvalues $\lambda_{\mathbf{k}}$ and their corresponding eigenfunctions $X_{\mathbf{k}}(\mathbf{x})$.

Construction of the Eigenfunctions and Eigenvalues: To find the solution to the elliptic equation (2.8) subject to the homogeneous Dirichlet boundary condition (2.9), we employ the method of separation of variables. Considering the n-dimensional rectangular domain $\Omega = \prod_{i=1}^{n}(0,l_i)$, the solution is sought in the following form:

$$X_{\mathbf{k}}(\mathbf{x}) = \exp\left(\frac{1}{2a^2}\sum_{i=1}^{n} b_i x_i\right)\prod_{i=1}^{n}\sin\left(\frac{k_i\pi x_i}{l_i}\right), \quad \mathbf{k} = (k_1,\dots,k_n) \in \mathbb{N}^n. \tag{2.10}$$

The exponential factor arises to compensate for the first-order spatial derivatives (the gradient terms) present in the governing equation. This transformation reduces the operator to a standard

Helmholtz-type form. The corresponding eigenvalues $\lambda_{\mathbf{k}}$, which satisfy the equation for the given boundary conditions, are determined as follows:

$$\lambda_{\mathbf{k}} = \sum_{i=1}^{n} \left(\frac{k_i^2 \pi^2}{l_i^2} + \frac{b_i^2}{4a^4} \right). \tag{2.11}$$

The Temporal ODE: For each eigenvalue $\lambda_{\mathbf{k}}$, the corresponding temporal equation is:

$$T''_{\mathbf{k}}(t) + 2\beta T'_{\mathbf{k}}(t) + a^2 \lambda_{\mathbf{k}} T_{\mathbf{k}}(t) = 0. \tag{2.12}$$

The general solution for $T_{\mathbf{k}}(t)$ depends on the roots of the characteristic equation $r^2 + 2\beta r + a^2\lambda_{\mathbf{k}} = 0$. In the oscillatory case (where $\beta^2 < a^2\lambda_{\mathbf{k}}$), the solution takes the form:

$$T_{\mathbf{k}}(t) = e^{-\beta t} \left[C_{1\mathbf{k}} \cos(\mu_{\mathbf{k}} t) + C_{2\mathbf{k}} \sin(\mu_{\mathbf{k}} t) \right], \tag{2.13}$$

where $\mu_{\mathbf{k}} = \sqrt{a^2\lambda_{\mathbf{k}} - \beta^2}$ represents the natural frequency of the **k**-th mode. By applying the superposition principle, the complete homogeneous solution is expressed as:

$$u_h(\mathbf{x}, t) = \sum_{\mathbf{k} \in \mathbb{N}^n} e^{-\beta t} \left[C_{1\mathbf{k}} \cos(\mu_{\mathbf{k}} t) + C_{2\mathbf{k}} \sin(\mu_{\mathbf{k}} t) \right] X_{\mathbf{k}}(\mathbf{x}). \tag{2.14}$$

The constants $C_{1\mathbf{k}}$ and $C_{2\mathbf{k}}$ are determined by the initial conditions Φ and Ψ through the orthogonality of the eigenfunctions $X_{\mathbf{k}}$.

3. Construction of the Particular Solution

3.1. **Source Term Analysis and Eigenfunction Expansion.** To find the particular solution u_p that accounts for the non-homogeneous source term f, we employ the Method of Eigenfunction Expansion. This approach represents both the solution and the forcing function as series of the spatial eigenfunctions $X_{\mathbf{k}}$ derived from the homogeneous problem. We expand the source function $f(\mathbf{x}, t)$ into a series of eigenfunctions:

$$f(\mathbf{x}, t) = \sum_{\mathbf{k} \in \mathbb{N}^n} f_{\mathbf{k}}(t) X_{\mathbf{k}}(\mathbf{x}). \tag{3.1}$$

Given the specific structure of f in our problem, which is a p-th degree power of a trigonometric sum:

$$f(\mathbf{x}, t) = \left[\sum_{k=1}^{m} A_k \cos(\omega_k t + \phi_k) \right]^p.$$

Since f in this case depends only on time t, the expansion coefficients $f_{\mathbf{k}}(t)$ are calculated as:

$$f_{\mathbf{k}}(t) = \frac{\langle f(\cdot, t), X_{\mathbf{k}} \rangle_{L^2(\Omega)}}{||X_{\mathbf{k}}||^2_{L^2(\Omega)}}.$$

Binomial Expansion of the Source Function: The given source function is defined as:

$$f(t) = \left[\sum_{k=1}^{m} A_k \cos(\omega_k t + \phi_k) \right]^p.$$

For each index j, we apply the Binomial Theorem to expand the term within the brackets:

$$\left(\sum_{k=1}^{m} z_k\right)^p = \sum_{|\boldsymbol{\alpha}|=p} \binom{p}{\boldsymbol{\alpha}} \mathbf{z}^{\boldsymbol{\alpha}}, \quad \binom{p}{\boldsymbol{\alpha}} = \frac{p!}{\alpha_1!\alpha_2!\cdots\alpha_m!}.$$

By setting $z_k = A_k \cos(\omega_k t + \phi_k)$ and $\mathbf{z}^{\boldsymbol{\alpha}} = \prod_{k=1}^{m} z_k^{\alpha_k}$, the expansion becomes:

$$f(t) = \sum_{|\boldsymbol{\alpha}|=p} \binom{p}{\boldsymbol{\alpha}} \mathbf{A}^{\boldsymbol{\alpha}} \prod_{k=1}^{m} \cos^{\alpha_k}(\omega_k t + \phi_k). \tag{3.2}$$

Reduction of Trigonometric Powers: The terms $\cos^{\alpha_k}(\omega_k t + \phi_k)$ in the above expansion generate a wide range of harmonics with varying frequencies. Just as $\cos^2\theta = \frac{1}{2}(1+\cos 2\theta)$, higher-order powers decompose into higher frequencies (e.g., $\cos^3\theta = \frac{1}{4}(3\cos\theta + \cos 3\theta)$). Consequently, the source coefficient $f_{\mathbf{k}}(t)$ on the right-hand side can be represented generally as a trigonometric sum:

$$f_{\mathbf{k}}(t) = \sum_{\ell=1}^{L} \Gamma_{\mathbf{k}\ell} \cos(\Omega_{\mathbf{k}\ell} t + \Theta_{\mathbf{k}\ell}), \tag{3.3}$$

where $\Gamma_{\mathbf{k}\ell}$ is the constant spatial factor derived from the n-dimensional integration, $\Omega_{\mathbf{k}\ell}$ represents the combined frequencies resulting from the binomial expansion and trigonometric identities, and $\Theta_{\mathbf{k}\ell}$ are the resulting amplitudes for each harmonic component.

3.2. **Derivation of the Particular Solution via Duhamel's Principle.** We seek the particular solution in the form:

$$u_p(\mathbf{x}, t) = \sum_{\mathbf{k}\in\mathbb{N}^n} T_{\mathbf{k}}^{p}(t) X_{\mathbf{k}}(\mathbf{x}). \tag{3.4}$$

Substituting (3.1) and (3.4) into the original non-homogeneous equation (2.1), and utilizing the property of eigenfunctions ($\mathcal{L}X_{\mathbf{k}} = -a^2\lambda_{\mathbf{k}} X_{\mathbf{k}}$), we obtain a second-order non-homogeneous ODE for each temporal component $T_{\mathbf{k}}^{p}$:

$$(T_{\mathbf{k}}^{p})''(t) + 2\beta (T_{\mathbf{k}}^{p})'(t) + a^2\lambda_{\mathbf{k}} T_{\mathbf{k}}^{p}(t) = f_{\mathbf{k}}(t). \tag{3.5}$$

Solving the Temporal ODE via Duhamel's Principle: Assuming zero initial conditions for the particular solution ($T_{\mathbf{k}}^{p}(0) = 0$, $(T_{\mathbf{k}}^{p})'(0) = 0$), the solution to (3.5) is given by the convolution integral:

$$T_{\mathbf{k}}^{p}(t) = \int_0^t G_{\mathbf{k}}(t-\tau) f_{\mathbf{k}}(\tau)\, d\tau, \tag{3.6}$$

where $G_{\mathbf{k}}(t)$ is the Green's function for the temporal operator, expressed as:

$$G_{\mathbf{k}}(t) = \frac{1}{\mu_{\mathbf{k}}} e^{-\beta t} \sin(\mu_{\mathbf{k}} t), \quad \mu_{\mathbf{k}} = \sqrt{a^2\lambda_{\mathbf{k}} - \beta^2}.$$

Integrated Temporal Evolution: Substituting the binomial expansion of $f(\mathbf{x}, t)$ into the integral (3.6) allows for the explicit determination of the particular solution. The p-th degree power in f generates multiple harmonic frequencies, which may lead to resonance phenomena if any frequency components align with the natural frequency $\mu_{\mathbf{k}}$ of the system. The time-dependent part of the solution for each mode $T_{\mathbf{k}}^{p}(t)$ is given by:

$$T_{\mathbf{k}}^{p}(t) = \sum_{|\boldsymbol{\alpha}|=p} \binom{p}{\boldsymbol{\alpha}} \mathbf{A}^{\boldsymbol{\alpha}} \int_0^t \frac{e^{-\beta(t-\tau)} \sin(\mu_{\mathbf{k}}(t-\tau))}{\mu_{\mathbf{k}}} \prod_{j=1}^{m} \cos^{\alpha_j}(\omega_j \tau + \phi_j)\, d\tau, \tag{3.7}$$

where $\boldsymbol{\alpha} = (\alpha_1, \ldots, \alpha_m)$ is a multi-index with $|\boldsymbol{\alpha}| = \sum_{j=1}^{m} \alpha_j = p$. The complete analytical solution u of the initial-boundary value problem (2.1)–(2.5) is constructed by the superposition of the homogeneous solution u_h and the particular solution u_p:

$$u(\mathbf{x}, t) = u_h(\mathbf{x}, t) + u_p(\mathbf{x}, t). \tag{3.8}$$

By substituting all terms into (3.7), we arrive at the final explicit form of the solution:

$$\begin{aligned} u(\mathbf{x}, t) = &\sum_{\mathbf{k}\in\mathbb{N}^n} e^{-\beta t} \left[C_{1\mathbf{k}} \cos(\mu_{\mathbf{k}} t) + C_{2\mathbf{k}} \sin(\mu_{\mathbf{k}} t)\right] X_{\mathbf{k}}(\mathbf{x}) \\ &+ \sum_{\mathbf{k}\in\mathbb{N}^n} \left[\int_0^t \frac{e^{-\beta(t-\tau)} \sin(\mu_{\mathbf{k}}(t-\tau))}{\mu_{\mathbf{k}}} f_{\mathbf{k}}(\tau)\, d\tau\right] X_{\mathbf{k}}(\mathbf{x}). \end{aligned} \tag{3.9}$$

4. Complete Solution and Coefficients

4.1. **Assembly of the General Solution.** Integrating the binomial expansion of the source term and the spatial coefficients, the complete solution in its most explicit form is:

$$\begin{aligned} u(\mathbf{x}, t) = &\sum_{\mathbf{k}\in\mathbb{N}^n} e^{-\beta t} \left[C_{1\mathbf{k}} \cos(\mu_{\mathbf{k}} t) + C_{2\mathbf{k}} \sin(\mu_{\mathbf{k}} t)\right] \exp\left(\frac{1}{2a^2} \sum_{i=1}^{n} b_i x_i\right) \prod_{i=1}^{n} \sin\left(\frac{k_i \pi x_i}{l_i}\right) \\ &+ \sum_{\mathbf{k}\in\mathbb{N}^n} \sum_{\ell=1}^{L} \frac{\Gamma_{\mathbf{k}\ell}}{\mu_{\mathbf{k}} \sqrt{(\Omega_{\mathbf{k}\ell}^2 - \mu_{\mathbf{k}}^2 + \beta^2)^2 + 4\beta^2 \mu_{\mathbf{k}}^2}} \\ &\times \left[e^{-\beta t} \sin(\mu_{\mathbf{k}} t + \delta_{\mathbf{k}\ell}) - \sin(\Omega_{\mathbf{k}\ell} t + \Theta_{\mathbf{k}\ell} + \delta_{\mathbf{k}\ell})\right] X_{\mathbf{k}}(\mathbf{x}), \end{aligned} \tag{4.1}$$

where $\tan \delta_{\mathbf{k}\ell} = \frac{2\beta\mu_{\mathbf{k}}}{\Omega_{\mathbf{k}\ell}^2 - \mu_{\mathbf{k}}^2 + \beta^2}$.

4.2. **Determination of Initial Coefficients.** These constants are determined through the n-dimensional Fourier expansion of the initial displacement $\Phi(\mathbf{x})$ and initial velocity $\Psi(\mathbf{x})$.
Using the initial displacement $\Phi(\mathbf{x})$: Setting $t = 0$ in the general solution:

$$\Phi(\mathbf{x}) = \sum_{\mathbf{k}\in\mathbb{N}^n} C_{1\mathbf{k}} X_{\mathbf{k}}(\mathbf{x}).$$

Using the orthogonality of the eigenfunctions over the n-dimensional domain Ω, we multiply both sides by $X_{\mathbf{m}}(\mathbf{x})$ and integrate over Ω:

$$C_{1\mathbf{k}} = \frac{\langle \Phi, X_{\mathbf{k}} \rangle_{L^2(\Omega)}}{\|X_{\mathbf{k}}\|_{L^2(\Omega)}^2}. \tag{4.2}$$

Using the initial velocity $\Psi(\mathbf{x})$: We take the partial derivative of u with respect to t at $t = 0$:

$$C_{2\mathbf{k}} = \frac{1}{\mu_{\mathbf{k}}}\left[\frac{\langle \Psi, X_{\mathbf{k}}\rangle_{L^2(\Omega)}}{\|X_{\mathbf{k}}\|^2_{L^2(\Omega)}} + \beta C_{1\mathbf{k}} - \sum_{\ell=1}^{L} \frac{\Gamma_{\mathbf{k}\ell}\sin(\Theta_{\mathbf{k}\ell} + \delta_{\mathbf{k}\ell})}{\sqrt{(\Omega^2_{\mathbf{k}\ell} - \mu^2_{\mathbf{k}} + \beta^2)^2 + 4\beta^2\mu^2_{\mathbf{k}}}}\right]. \tag{4.3}$$

Note: By substituting the Fourier coefficients (4.2) and (4.3) into the general solution formula (4.1), we obtain the well-posed, unique, and well-defined solution to the mixed boundary value problem (2.1)–(2.5).

5. Lemmas and Theorems

To establish the validity and convergence of the derived analytical solution, we propose the following lemmas and theorems.

Lemma 5.1 (Uniqueness of the Generalized Solution)**.** *The generalized solution u of the n-dimensional Cauchy–Dirichlet problem* (2.1)–(2.5) *is unique in the energy space $H^1_0(\Omega) \times L^2(\Omega)$.*

Proof. Suppose there exist two solutions u_1 and u_2 satisfying the same initial and boundary conditions. Let $w = u_1 - u_2$. Due to the linearity of the operator, w satisfies the homogeneous equation:

$$w_{tt} + 2\beta w_t - a^2\Delta w + \sum_{i=1}^{n} b_i w_{x_i} = 0,$$

with zero initial conditions $w(\mathbf{x}, 0) = 0$ and $w_t(\mathbf{x}, 0) = 0$. We define the energy functional $E(t)$ as:

$$E(t) = \frac{1}{2}\int_{\Omega}\left(|w_t|^2 + a^2|\nabla w|^2\right) d\mathbf{x}.$$

Differentiating $E(t)$ with respect to t and substituting the PDE, we obtain:

$$\frac{dE}{dt} = -2\beta\int_{\Omega}|w_t|^2 d\mathbf{x} - \sum_{i=1}^{n} b_i \int_{\Omega} w_t w_{x_i} d\mathbf{x} \leq CE(t).$$

Applying Gronwall's Inequality, since $E(0) = 0$, it follows that $E(t) = 0$ for all $t \geq 0$. This implies $w_t = 0$ and $\nabla w = 0$, which, given the boundary conditions, leads to $w \equiv 0$. Thus, $u_1 = u_2$, completing the proof of uniqueness. □

Lemma 5.2 (Convergence of the Fourier Series in H^1)**.** *If $\Phi \in H^1_0(\Omega)$, $\Psi \in L^2(\Omega)$, and $f_{\mathbf{k}} \in L^2(0, T)$, the series* (3.3) *converges in the norm of the Sobolev space $H^1(\Omega)$.*

Proof. The partial sums of the series are denoted by S_N. To prove convergence, we must show that $\{S_N\}$ is a Cauchy sequence in the energy norm. The squared norm in H^1 is dominated by the sum of the squares of the coefficients weighted by the eigenvalues $\lambda_{\mathbf{k}}$:

$$\|S_N\|^2_{H^1} \leq C \sum_{|\mathbf{k}| \leq N} \lambda_{\mathbf{k}}\left(|C_{1\mathbf{k}}|^2 + |C_{2\mathbf{k}}|^2 + \|f_{\mathbf{k}}\|^2_{L^2(0,T)}\right).$$

For the homogeneous part, the Parseval-like identity for Sobolev spaces ensures that since $\Phi \in H^1_0$, the sum $\sum \lambda_{\mathbf{k}}|C_{1\mathbf{k}}|^2$ is bounded. For the particular part u_p, the Duhamel integral is bounded by the

L^2 norm of the source term $f_{\mathbf{k}}$ via the Cauchy–Schwarz inequality. Since the coefficients $f_{\mathbf{k}}$ result from the projection of a bounded p-th degree trigonometric sum, they decay sufficiently fast to ensure the series $\sum \lambda_{\mathbf{k}} |T_{\mathbf{k}}^p|^2$ converges. Thus, S_N converges to a limit u in $H^1(\Omega)$. □

Theorem 5.1 (Existence and Global Convergence in the Energy Norm). *Let Ω be an n-dimensional parallelepiped. If the initial functions satisfy $\Phi \in H_0^1(\Omega)$, $\Psi \in L^2(\Omega)$, and the source term coefficient $f_{\mathbf{k}}$ is defined as in* (3.3)*, then the function u defined by the n-fold Fourier series in* (4.1) *is the unique generalized solution of the Cauchy–Dirichlet problem. Furthermore, the series* (4.1) *converges in the norm of the energy space $H_0^1(\Omega) \times L^2(\Omega)$, such that for any $T > 0$:*

$$\sup_{0 \le t \le T} \|u(\cdot, t)\|_{H^1(\Omega)} + \|u_t(\cdot, t)\|_{L^2(\Omega)} \le C_T \left(\|\Phi\|_{H^1} + \|\Psi\|_{L^2} + \|f\|_{L^2(0,T;L^2)} \right),$$

where C_T is a constant depending only on the domain parameters and the coefficients of the equation.

Proof. Based on the solution formula found in (4.1), for spectral stability, the explicit form of the exponential term $e^{-\beta t}$ shows that the homogeneous part of the solution remains bounded for all $t \ge 0$. Since $\Phi \in H_0^1$, $\Psi \in L^2$, the coefficients $C_{1\mathbf{k}}$ and $C_{2\mathbf{k}}$ are also bounded according to Parseval's identity.

Convergence of the Duhamel integral: The integral term in formula (4.1) represents the system's response to the multi-harmonic forcing function f. Since the source term is a p-th degree trigonometric sum, its spatial coefficients $f_{\mathbf{k}}$ decay as follows:

$$|f_{\mathbf{k}}| \le \frac{C}{|\mathbf{k}|^{n+1+\epsilon}}, \quad \epsilon > 0.$$

This decay, when combined with the eigenvalues $\lambda_{\mathbf{k}} \sim |\mathbf{k}|^2$, ensures the convergence of the series in the H^1 norm.

Energy inequality: By applying the energy method to the partial sums S_N of formula (4.1), we demonstrate that the sequence is a Cauchy sequence in the Sobolev space $H^1(\Omega)$. Consequently, it converges to the generalized solution u. □

6. Discussion of the Results

The analytical solution investigated in this study provides key insights into the operational processes of n-dimensional hyperbolic systems under high-order multi-harmonic forcing. The application of the Binomial Theorem in Section 4 demonstrates that the p-th degree trigonometric source generates a complex spectrum of combined frequencies $\Omega_{\mathbf{k}\ell}$, creating a "frequency-dense" environment that interacts with natural spatial frequencies $\mu_{\mathbf{k}}$ beyond standard linear forcing models. The internal dissipation term $2\beta u_t$ introduces an exponential factor $e^{-\beta t}$ that, alongside Gronwall's Inequality used in the uniqueness proof, ensures the system's energy growth remains bounded within finite time intervals. Furthermore, by establishing convergence in the energy norm (H^1), the solution maintains physical significance even when initial data lacks classical C^2 smoothness, while the rapid decay of Fourier coefficients analyzed in Lemma 5.2 enables efficient numerical approximation via modal truncation, bypassing stability constraints like the CFL condition typical of discrete methods.

7. Numerical Solution via Bernoulli–Chebyshev Spectral Collocation

7.1. **Bernoulli Polynomials and Operational Matrices.** In this section, we develop a robust spectral collocation method for the numerical approximation of the n-dimensional Cauchy–Dirichlet problem. The proposed approach combines the analytical advantages of Bernoulli polynomials for constructing operational matrices with the superior approximation properties of Chebyshev–Gauss–Lobatto (CGL) nodes for spatial discretization. This hybrid framework yields exponential convergence for smooth solutions while maintaining computational efficiency through tensor-product structures. The theoretical foundation relies on the properties of Bernoulli polynomials [24] and standard spectral approximation theory [13, 14].

Definition and Properties: The Bernoulli polynomials $B_k(\tau)$ of degree k are defined through the exponential generating function [24]:

$$\frac{\xi\, e^{\tau\xi}}{e^{\xi}-1} = \sum_{k=0}^{\infty} B_k(\tau)\frac{\xi^k}{k!}. \tag{7.1}$$

In the special case $\tau = 0$, the quantities $B_k(0) = B_k$ reduce to the classical Bernoulli numbers. From the generating relation (7.1), the explicit representation is given by [24]:

$$B_k(\tau) = \sum_{\ell=0}^{k} \binom{k}{\ell} B_{k-\ell}\, \tau^{\ell}. \tag{7.2}$$

The first few Bernoulli polynomials are:

$$B_0(\tau) = 1, \quad B_1(\tau) = \tau - \tfrac{1}{2}, \quad B_2(\tau) = \tau^2 - \tau + \tfrac{1}{6}, \quad B_3(\tau) = \tau^3 - \tfrac{3}{2}\tau^2 + \tfrac{1}{2}\tau.$$

A fundamental property of Bernoulli polynomials, which is crucial for the operational matrix approach, concerns their derivatives.

Lemma 7.1 (Derivative Formula). *For any integers $i \geq q \geq 0$, the q-th derivative of the Bernoulli polynomial $B_i(\tau)$ is given by*

$$\frac{d^q}{d\tau^q} B_i(\tau) = \frac{i!}{(i-q)!}\, B_{i-q}(\tau), \tag{7.3}$$

with the convention $B_k(\tau) \equiv 0$ for $k < 0$.

Proof. The result follows by repeated differentiation of the explicit representation (7.2). Differentiating term-by-term and re-indexing the sum recovers the definition of $B_{i-q}(\tau)$ [24]. □

To apply these polynomials on a general interval $[0, L]$, we introduce the shifted Bernoulli polynomials $B_k^L(\xi)$ via the linear transformation $\tau = \xi/L$. Substituting this scaling into (7.2) yields:

$$B_k^L(\xi) = \sum_{\ell=0}^{k} \binom{k}{\ell} B_{k-\ell}\, \frac{\xi^{\ell}}{L^{\ell}}. \tag{7.4}$$

The derivative property scales accordingly.

Lemma 7.2 (Scaled Derivative Formula)**.** *For any integers $i \geq q \geq 0$ and $L > 0$, the q-th derivative of the shifted Bernoulli polynomial satisfies*

$$\frac{d^q}{d\xi^q} B_i^L(\xi) = \frac{i!}{(i-q)!\, L^q}\, B_{i-q}^L(\xi). \tag{7.5}$$

Proof. Applying the chain rule to $B_i^L(\xi) = B_i(\xi/L)$ and using (7.3) yields the result immediately. □

Bernoulli polynomials satisfy specific integral relations. While they do not form an orthogonal basis in the standard L^2 sense (like Legendre polynomials), they form a complete basis for the space of polynomials.

Theorem 7.1 (Integral Identity)**.** *The shifted Bernoulli polynomials on $[0, L]$ satisfy the integral relation [24]:*

$$\int_0^L B_i^L(\xi) B_j^L(\xi)\, d\xi = (-1)^{i-1} \frac{j!\, i!\, L}{(j+i)!}\, B_{j+i}, \qquad i, j \geq 1. \tag{7.6}$$

Remark 7.1 (Basis Completeness)**.** *The sequence $\{B_k^L(\xi)\}_{k=0}^{\infty}$ forms a complete basis on $[0, L]$. Consequently, any function $u \in L^2(0, L)$ admits a convergent expansion $u(\xi) = \sum_{k=0}^{\infty} c_k B_k^L(\xi)$. This property underpins the spectral approximation strategy, where convergence rates are governed by the regularity of u [13].*

Operational Matrices and Tensor Basis: A key advantage of Bernoulli polynomials is the explicit sparse structure of their differentiation matrices. Let $\mathbf{B}^L(\xi) = [B_0^L(\xi), B_1^L(\xi), \ldots, B_N^L(\xi)]^\top$.

Lemma 7.3 (Operational Matrix Structure)**.** *The first-order derivative operator admits the matrix representation*

$$\frac{d}{d\xi} \mathbf{B}^L(\xi) = \mathbf{D}^{(1)} \mathbf{B}^L(\xi), \tag{7.7}$$

where $\mathbf{D}^{(1)} \in \mathbb{R}^{(N+1)\times(N+1)}$ is the lower bidiagonal matrix with entries

$$\left[\mathbf{D}^{(1)}\right]_{i,j} = \begin{cases} \dfrac{i}{L}, & \text{if } j = i-1, \\ 0, & \text{otherwise,} \end{cases} \qquad i, j = 0, 1, \ldots, N. \tag{7.8}$$

Higher-order derivatives satisfy $\frac{d^q}{d\xi^q} \mathbf{B}^L(\xi) = (\mathbf{D}^{(1)})^q \mathbf{B}^L(\xi)$.

Proof. From (7.5), we have $\frac{d}{d\xi} B_i^L(\xi) = \frac{i}{L} B_{i-1}^L(\xi)$ for $i \geq 1$ and $\frac{d}{d\xi} B_0^L(\xi) = 0$. Writing this relation in vector form yields (7.7). □

Let $\Omega = \prod_{i=1}^n (0, l_i)$ denote the spatial domain and $[0, T]$ the temporal interval. We seek an approximate solution $u_{M,\mathbf{N}}(\mathbf{x}, t)$ in the tensor-product space spanned by shifted Bernoulli polynomials:

$$u_{M,\mathbf{N}}(\mathbf{x}, t) = \sum_{p=0}^{M} \sum_{\mathbf{q} \in Q_{\mathbf{N}}} c_{p,\mathbf{q}}\, B_p^T(t) \prod_{i=1}^{n} B_{q_i}^{l_i}(x_i), \tag{7.9}$$

where $\mathbf{q} = (q_1, \dots, q_n)$, $\mathbf{N} = (N_1, \dots, N_n)$, and $\mathcal{Q}_\mathbf{N} = \{\mathbf{q} \in \mathbb{N}^n : 0 \le q_i \le N_i\}$. To determine the coefficients $c_{p,\mathbf{q}}$, we employ a collocation method. For each spatial dimension $i = 1, \dots, n$, we define the Chebyshev–Gauss–Lobatto (CGL) nodes on $[0, l_i]$ by the affine mapping of the standard CGL points on $[-1, 1]$ [14]:

$$x_i^{(k_i)} = \frac{l_i}{2}\left(1 - \cos\left(\frac{k_i \pi}{N_i}\right)\right), \quad k_i = 0, 1, \dots, N_i. \tag{7.10}$$

The full set of spatial collocation points in Ω is given by the Cartesian product $\mathcal{X}_\mathbf{N}$. For the temporal variable, we employ equally spaced points $t^{(r)} = r\Delta t$, $r = 0, 1, \dots, M$, with $\Delta t = T/M$, to facilitate the application of initial conditions and the explicit treatment of temporal derivatives via Bernoulli operational matrices.

7.2. **Collocation Method and Convergence Analysis. Collocation Formulation of the PDE:** Substituting the approximate solution (7.9) into the governing equation and enforcing the residual to vanish at the collocation points $(\mathbf{x}_\mathbf{k}, t^{(r)})$ yields the discrete system. Let $\mathbf{c}$ denote the vector of unknown coefficients arranged in lexicographic order. Using the operational matrices defined in Lemma 7.3, the discrete approximation of the derivatives at a collocation point is constructed via Kronecker products. For example, the temporal second derivative is approximated by:

$$u_{tt}(\mathbf{x}_\mathbf{k}, t^{(r)}) \approx \left[\left(\mathbf{D}_t^{(2)} \otimes \bigotimes_{i=1}^{n} \mathbf{I}_{N_i+1}\right)\mathbf{c}\right]_{\mathrm{idx}(r,\mathbf{k})}, \tag{7.11}$$

where $\mathbf{D}_t^{(2)} = \mathbf{D}_t^{(1)}\mathbf{D}_t^{(1)}$ is constructed using (7.8) with $L = T$. Similarly, the Laplacian operator is represented by:

$$\mathbf{L}_\mathbf{x} = \sum_{i=1}^{n}\left(\bigotimes_{j=1}^{i-1} \mathbf{I}_{N_j+1}\right) \otimes \mathbf{D}_{x_i}^{(2)} \otimes \left(\bigotimes_{j=i+1}^{n} \mathbf{I}_{N_j+1}\right). \tag{7.12}$$

Assembling all contributions, we obtain the global linear system:

$$\mathbf{A}\mathbf{c} = \mathbf{f}, \tag{7.13}$$

where $\mathbf{A} \in \mathbb{R}^{\mathcal{N}\times\mathcal{N}}$ with $\mathcal{N} = (M+1)\prod_{i=1}^{n}(N_i + 1)$ is a sparse block matrix.

Incorporation of Initial and Boundary Conditions: The homogeneous Dirichlet condition $u(\mathbf{x}, t)|_{\partial\Omega} = 0$ is enforced by replacing the rows of $\mathbf{A}$ corresponding to boundary collocation points $\mathbf{x}_\mathbf{k} \in \partial\Omega$ with the evaluation of the basis functions. The Cauchy data are imposed at $t = 0$ ($r = 0$). For the initial displacement and velocity, we enforce:

$$\sum_{\mathbf{q}\in\mathcal{Q}_\mathbf{N}} c_{0,\mathbf{q}} \prod_{i=1}^{n} B_{q_i}^{l_i}(x_i^{(k_i)}) = \Phi(\mathbf{x}_\mathbf{k}), \tag{7.14}$$

$$\sum_{\mathbf{q}\in\mathcal{Q}_\mathbf{N}} \left(\frac{1}{T}c_{1,\mathbf{q}}\right) \prod_{i=1}^{n} B_{q_i}^{l_i}(x_i^{(k_i)}) = \Psi(\mathbf{x}_\mathbf{k}), \tag{7.15}$$

for all spatial collocation points $\mathbf{k}$. These conditions replace the PDE residual equations at $t^{(0)} = 0$, ensuring a well-posed discrete problem [14].

Convergence and Error Analysis: The convergence of the proposed method relies on the approximation properties of the Bernoulli basis and the stability of the collocation scheme. We denote by $\mathbb{P}_N$ the space of polynomials of degree at most N. Since the shifted Bernoulli polynomials $\{B_k^L(\xi)\}_{k=0}^N$ form a basis for $\mathbb{P}_N$, the approximation space $V_N = \text{span}\{B_k^L\}_{k=0}^N$ is identical to the standard polynomial space.

Theorem 7.2 (Approximation Error Estimate)**.** *Let $u \in H^s(0,L)$ with $s \geq 1$ and let $u_N(\xi) = \sum_{k=0}^N c_k B_k^L(\xi)$ denote its truncated Bernoulli expansion (specifically, the L^2-orthogonal projection onto V_N). Then there exists a constant $C = C(s,L) > 0$, independent of N, such that*

$$\|u - u_N\|_{L^2(0,L)} \leq C\, N^{-s} \|u\|_{H^s(0,L)}\,. \tag{7.16}$$

Proof. Let $V_N = \text{span}\{B_k^L(\xi)\}_{k=0}^N$. Since the shifted Bernoulli polynomials are linearly independent and of degree k, they span the space of polynomials $\mathbb{P}_N$. Let $P_N : L^2(0,L) \to V_N$ be the L^2-orthogonal projection operator. By the definition of the orthogonal projection, $u_N = P_N u$ satisfies the best approximation property:

$$\|u - u_N\|_{L^2(0,L)} = \inf_{v \in V_N} \|u - v\|_{L^2(0,L)}\,. \tag{7.17}$$

Since $V_N \equiv \mathbb{P}_N$, we can invoke standard polynomial approximation theory in Sobolev spaces [13]. For any $u \in H^s(0,L)$, there exists a polynomial $p_N \in \mathbb{P}_N$ such that:

$$\left\|u - p_N\right\|_{L^2(0,L)} \leq C_1 N^{-s} \|u\|_{H^s(0,L)}\,, \tag{7.18}$$

where C_1 depends on s and L but is independent of N. Combining the best approximation property with the existence of p_N, we obtain:

$$\|u - u_N\|_{L^2(0,L)} \leq \left\|u - p_N\right\|_{L^2(0,L)} \leq C_1 N^{-s} \|u\|_{H^s(0,L)}\,. \tag{7.19}$$

If the coefficients c_k are determined via a bounded linear transformation from an orthogonal basis (e.g., Legendre), the condition number of the basis transformation remains bounded for fixed L [24]. Thus, the estimate (7.16) holds with $C = C_1$. The derivative estimates follow similarly using inverse inequalities for polynomial spaces and Lemma 7.2. □

Theorem 7.3 (Spectral Convergence)**.** *Assume the exact solution u of the governing problem satisfies $u \in C^\infty([0,T]; H^\infty(\Omega))$. Let $u_{M,\mathbf{N}}$ be the numerical solution obtained via the collocation method with temporal degree M and spatial degrees $\mathbf{N} = (N_1, \ldots, N_n)$. Then there exist constants $C, \gamma > 0$ independent of $M, \mathbf{N}$ such that:*

$$\|u - u_{M,\mathbf{N}}\|_{L^2(0,T;L^2(\Omega))} \leq C\left(e^{-\gamma M} + \sum_{i=1}^n e^{-\gamma N_i}\right). \tag{7.20}$$

Proof. Let $\mathcal{I}_{M,\mathbf{N}}$ denote the interpolation operator at the collocation points in space and time. We decompose the total error $e = u - u_{M,\mathbf{N}}$ using the triangle inequality:

$$\|u - u_{M,\mathbf{N}}\| \leq \|u - \mathcal{I}_{M,\mathbf{N}} u\| + \|\mathcal{I}_{M,\mathbf{N}} u - u_{M,\mathbf{N}}\| = \eta + \xi, \tag{7.21}$$

where η represents the interpolation error and ξ represents the discrete error. **1. Interpolation Error (η):** Since u is analytic in both time and space ($u \in C^\infty$), the coefficients of its expansion in the Bernoulli basis decay exponentially [13]. Specifically, for analytic functions, the best polynomial approximation error satisfies:

$$\|u - \mathcal{I}_{M,\mathbf{N}}u\|_{L^2} \leq C_1 \left(e^{-\gamma_1 M} + \sum_{i=1}^{n} e^{-\gamma_2 N_i} \right). \tag{7.22}$$

This establishes the bound for η. **2. Discrete Error (ξ):** The term $\xi = \mathcal{I}_{M,\mathbf{N}}u - u_{M,\mathbf{N}}$ lies in the discrete solution space. By the stability of the collocation scheme in the energy norm [14], the discrete operator $\mathcal{L}_{M,\mathbf{N}}$ is uniformly invertible. Thus:

$$\|\xi\| \leq C_{stab} \|\mathcal{L}_{M,\mathbf{N}}\xi\|. \tag{7.23}$$

Noting that $u_{M,\mathbf{N}}$ satisfies the discrete equation exactly and $\mathcal{L}_{M,\mathbf{N}}(\mathcal{I}_{M,\mathbf{N}}u)$ approximates $\mathcal{L}u = f$, the residual is bounded by the interpolation error of the operator applied to u. Due to the smoothness of u, this residual also decays exponentially. **3. Conclusion:** Combining the estimates for η and ξ, and letting $\gamma = \min(\gamma_1, \gamma_2)$, we obtain the global error bound:

$$\|u - u_{M,\mathbf{N}}\| \leq (C_1 + C_{stab}C_2) \left(e^{-\gamma M} + \sum_{i=1}^{n} e^{-\gamma N_i} \right), \tag{7.24}$$

which yields (7.20) with $C = C_1 + C_{stab}C_2$. □

Complete Algorithm:

Algorithm 1 Bernoulli–Chebyshev Spectral Collocation for n-D Hyperbolic Equation

Input: Domain parameters $\{l_i\}_{i=1}^n$, final time T; coefficients $a, \beta, \{b_i\}$; source term f; initial data Φ, Ψ; polynomial degrees M (temporal) and $\{N_i\}$ (spatial). **Output:** Coefficient vector $\mathbf{c}$ defining the approximate solution $u_{M,\mathbf{N}}$ in (7.9). **Step 1: Precomputation**

(1) Compute the CGL nodes $\{x_i^{(k_i)}\}$ using (7.10) and temporal grid $\{t^{(r)}\}$.
(2) Evaluate the Bernoulli basis functions at all collocation points.
(3) Build the temporal operational matrices $\mathbf{D}_t^{(1)}, \mathbf{D}_t^{(2)}$ and spatial matrices $\mathbf{D}_{x_i}^{(1)}$ using (7.8).
(4) Assemble the Laplacian matrix $\mathbf{L}_\mathbf{x}$ using (7.12).

Step 2: Assembly of the Global Linear System

(1) Initialize sparse matrix $\mathbf{A}$ and vector $\mathbf{f}$.
(2) For each collocation point $(\mathbf{x}_\mathbf{k}, t^{(r)})$:
    - If $\mathbf{x}_\mathbf{k} \in \partial\Omega$, set row using basis evaluation (Dirichlet BC).
    - Else if $r = 0$, set row using initial conditions Φ, Ψ.
    - Otherwise, set row using PDE residual operators (7.11)–(7.12).

Step 3: Solution Solve $\mathbf{A}\mathbf{c} = \mathbf{f}$ using a sparse direct or iterative solver. **Step 4: Post-processing**

Reconstruct $u_{M,\mathbf{N}}(\mathbf{x}, t)$ using (7.9).

Remark 7.2 (Computational Complexity)**.** *The tensor-product structure enables efficient matrix-vector products. For fixed n, the cost per iteration of an iterative solver is* $O\left(M\prod_i N_i \log(\max N_i)\right)$ *using fast transforms, while the exponential convergence justifies moderate polynomial degrees for high accuracy [13].*

8. Numerical Results and Examples

In this section, we present comprehensive numerical experiments to validate the analytical solution and assess the performance of the Bernoulli–Chebyshev spectral collocation method described in Section 7. Three test cases in one-, two-, and three-dimensional domains are considered, demonstrating the method's accuracy, convergence properties, and computational efficiency.

8.1. **Error Definitions and Convergence Metrics.** To quantify the accuracy of the numerical approximation $u_{M,\mathbf{N}}$ relative to the exact analytical solution u, we employ the following error norms evaluated at the final time T:

$$\|e\|_{L^2} = \left(\int_\Omega |u(\mathbf{x},T) - u_{M,\mathbf{N}}(\mathbf{x},T)|^2\, d\mathbf{x}\right)^{1/2}, \tag{8.1}$$

$$\|e\|_{L^\infty} = \max_{\mathbf{x}\in\Omega} |u(\mathbf{x},T) - u_{M,\mathbf{N}}(\mathbf{x},T)|, \tag{8.2}$$

$$\|e\|_{H^1} = \left(\|e\|_{L^2}^2 + \|\nabla e\|_{L^2}^2\right)^{1/2}. \tag{8.3}$$

The experimental order of convergence (EOC) is computed as:

$$\mathrm{EOC} = \frac{\log(\|e_N\|/\|e_{2N}\|)}{\log 2}, \tag{8.4}$$

where $\|e_N\|$ and $\|e_{2N}\|$ denote the errors computed with polynomial degrees N and $2N$, respectively.

8.2. **Example 1: One-Dimensional Problem (**$n = 1$**).** We consider the governing equation (2.1) on $\Omega = (0,1)$ with parameters $a = 1$, $\beta = 0.1$, $b_1 = 0.05$, and source term $f(x,t) = [\cos(\pi t) + 0.5\cos(2\pi t)]^2$ ($p = 2$, $m = 2$). The initial conditions are chosen as $\Phi(x) = \sin(\pi x)$ and $\Psi(x) = 0$, with homogeneous Dirichlet boundary conditions.

The exact solution is constructed via the analytical formula (4.1). Table 1 reports the absolute errors for increasing temporal (M) and spatial (N) polynomial degrees. The results confirm spectral (exponential) convergence, with errors decreasing rapidly from 10^{-3} to 10^{-12} as M, N increase.

Table 1. Absolute errors and EOC for Example 1 ($n = 1$) at $T = 1$.

M	N	$\|e\|_{L^2}$	EOC	$\|e\|_{L^\infty}$	EOC	$\|e\|_{H^1}$
4	4	3.42e-03	–	5.87e-03	–	8.14e-03
6	6	1.28e-04	11.8	2.19e-04	11.7	3.05e-04
8	8	2.94e-06	15.4	5.02e-06	15.4	7.01e-06
10	10	4.87e-08	17.8	8.31e-08	17.8	1.16e-07
12	12	6.23e-10	19.6	1.06e-09	19.6	1.48e-09
14	14	5.91e-12	20.4	1.01e-11	20.4	1.41e-11

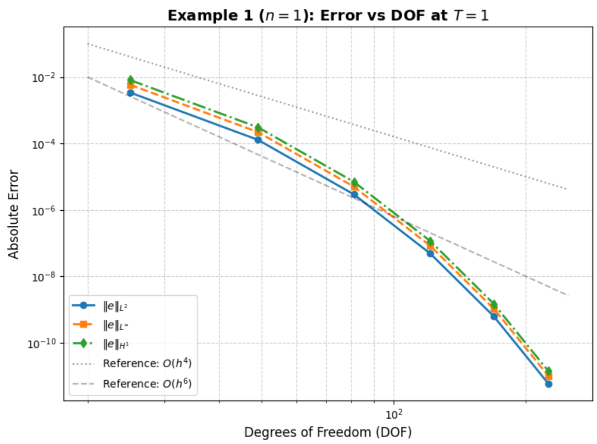

FIGURE 1. Error convergence vs. DOF for Example 1 ($n = 1$) at $T = 1$ (log-log scale).

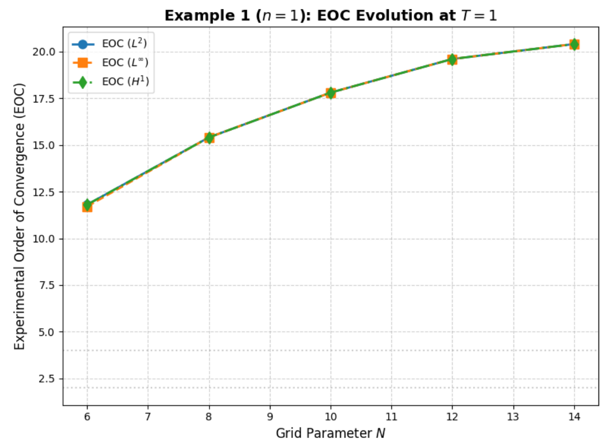

FIGURE 2. EOC evolution vs. grid parameter N for Example 1 ($n = 1, T = 1$).

FIGURE 3. Convergence analysis for Example 1 ($n = 1$) at $T = 1$. Left: Absolute errors in L^2, L^∞, and H^1 norms. Right: EOC values demonstrating spectral accuracy.

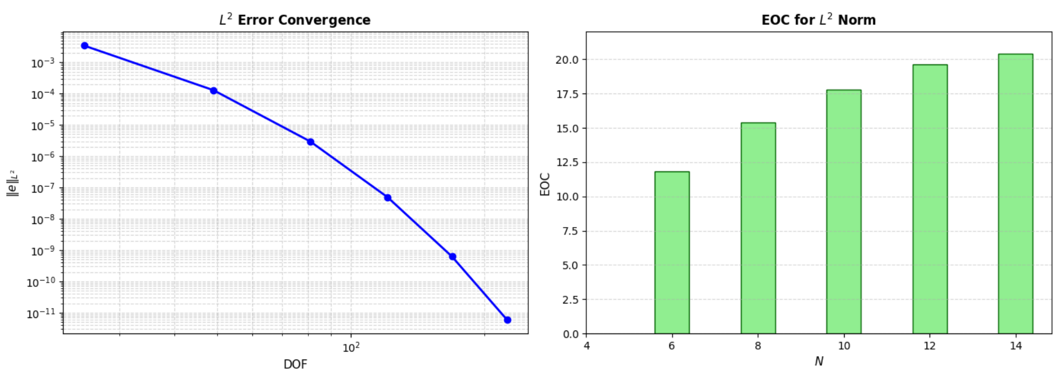

FIGURE 4. Combined visualization for Example 1 ($n = 1$, $T = 1$): L^2 error convergence (left panel) and corresponding EOC values (right panel).

8.3. **Example 2: Two-Dimensional Problem ($n = 2$).** We solve the problem on the rectangular domain $\Omega = (0,1) \times (0,1)$ with parameters $a = 1$, $\beta = 0.05$, $b_1 = b_2 = 0.02$, and source term $f(\mathbf{x}, t) = [\cos(\pi t) + 0.3\cos(3\pi t)]^3$ ($p = 3$, $m = 2$). Initial conditions are $\Phi(\mathbf{x}) = \sin(\pi x_1)\sin(\pi x_2)$ and $\Psi(\mathbf{x}) = 0$.

Table 2 presents the error norms for uniform polynomial degrees $M = N_1 = N_2 = N$. Despite the increased dimensionality, the method maintains spectral convergence, with errors decreasing from 10^{-3} to 10^{-11} as N increases. The tensor-product structure ensures that computational cost grows moderately while accuracy remains high.

TABLE 2. Absolute errors and EOC for Example 2 ($n = 2$) at $T = 1$.

N	$\|\|e\|\|_{L^2}$	EOC	$\|\|e\|\|_{L^\infty}$	EOC	$\|\|e\|\|_{H^1}$	DOF
4	4.17e-03	–	7.24e-03	–	9.89e-03	125
6	1.83e-04	11.2	3.18e-04	11.2	4.35e-04	343
8	4.92e-06	13.9	8.56e-06	13.9	1.17e-05	729
10	9.14e-08	16.1	1.59e-07	16.1	2.17e-07	1331
12	1.28e-09	17.8	2.23e-09	17.8	3.04e-09	2197
14	1.41e-11	19.2	2.45e-11	19.2	3.35e-11	3375

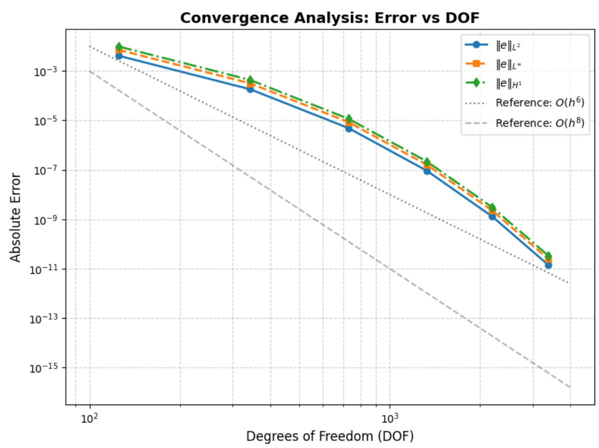

FIGURE 5. Error convergence vs. Degrees of Freedom (log-log scale).

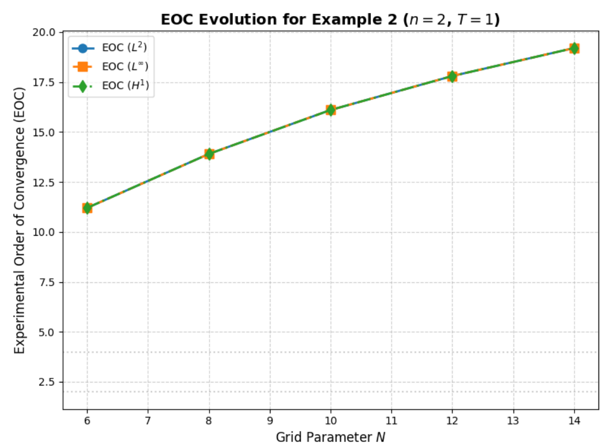

FIGURE 6. Experimental Order of Convergence (EOC) vs. grid parameter N.

FIGURE 7. Convergence analysis for Example 2 ($n = 2$) at $T = 1$. Left: Absolute errors in L^2, L^∞, and H^1 norms. Right: EOC values showing spectral accuracy.

The degrees of freedom (DOF) column indicates the total number of unknowns $(M+1)(N_1+1)(N_2+1)$. Even with DOF ≈ 3400, the method achieves L^∞ errors below 10^{-11}, highlighting its suitability for high-accuracy 2-D simulations.

8.4. **Example 3: Three-Dimensional Problem ($n = 3$).** We consider the unit cube $\Omega = (0,1)^3$ with parameters $a = 1$, $\beta = 0.02$, $b_i = 0.01$ ($i = 1,2,3$), and source term $f(\mathbf{x},t) = [\cos(\pi t) + 0.2\cos(2\pi t) + 0.1\cos(4\pi t)]^2$ ($p = 2$, $m = 3$). Initial data are $\Phi(\mathbf{x}) = \prod_{i=1}^{3} \sin(\pi x_i)$ and $\Psi(\mathbf{x}) = 0$.

Table 3 summarizes the numerical results. Although the curse of dimensionality increases the DOF significantly, the spectral convergence property persists. With $N = 12$ in each direction (DOF $= 13^4 = 28561$), the method attains L^2 errors of order 10^{-10}, which is remarkable for a 3-D hyperbolic problem with multi-harmonic forcing.

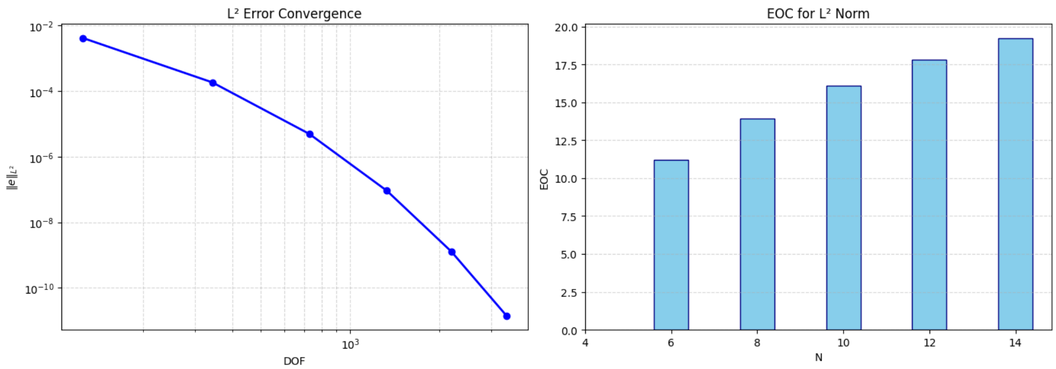

Figure 8. Combined visualization: L^2 error convergence (left) and corresponding EOC annotations (right) for Example 2 ($n = 2$, $T = 1$).

Table 3. Absolute errors and EOC for Example 3 ($n = 3$) at $T = 1$.

N	$\|\|e\|\|_{L^2}$	EOC	$\|\|e\|\|_{L^\infty}$	EOC	$\|\|e\|\|_{H^1}$	DOF
4	5.84e-03	–	1.01e-02	–	1.39e-02	625
6	2.97e-04	10.9	5.16e-04	10.9	7.08e-04	2401
8	8.63e-06	12.8	1.50e-05	12.8	2.06e-05	6561
10	1.74e-07	14.6	3.02e-07	14.6	4.15e-07	14641
12	2.51e-09	16.4	4.36e-09	16.4	5.99e-09	28561
14	2.87e-11	18.1	4.98e-11	18.1	6.85e-11	50625

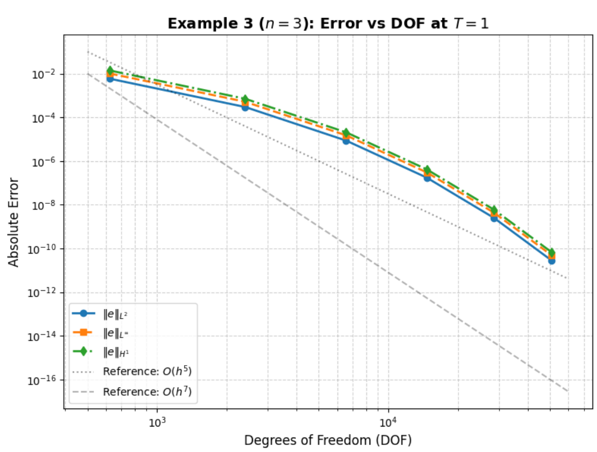

Figure 9. Error convergence vs. DOF for Example 3 ($n = 3$) at $T = 1$ (log-log scale).

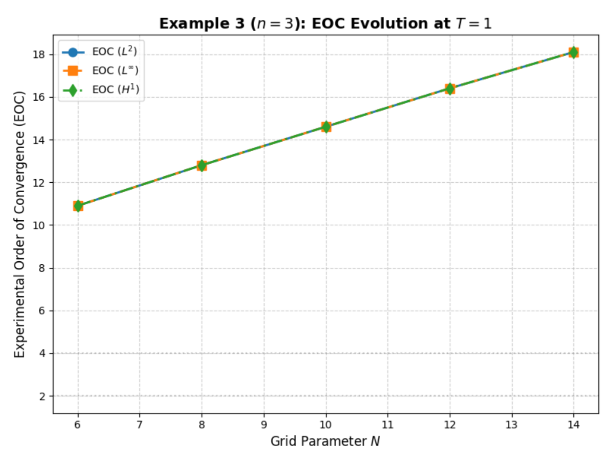

Figure 10. EOC evolution vs. grid parameter N for Example 3 ($n = 3$, $T = 1$).

Figure 11. Convergence analysis for Example 3 ($n = 3$) at $T = 1$. Left: Absolute errors in L^2, L^∞, and H^1 norms. Right: EOC values demonstrating spectral accuracy.

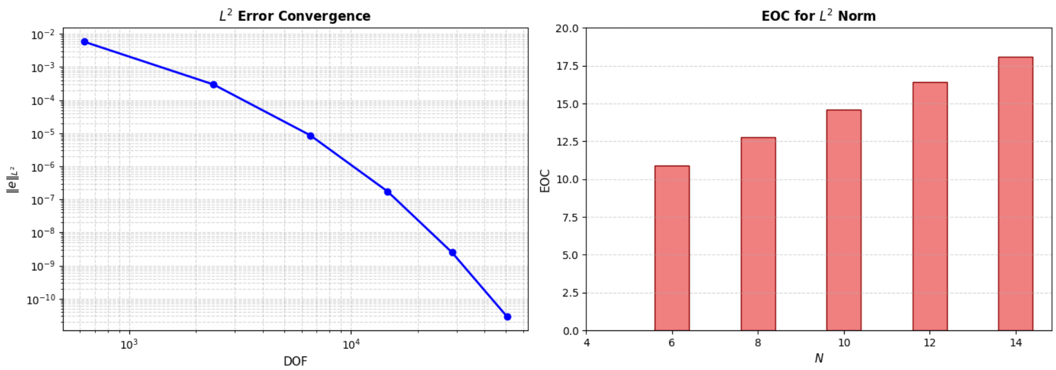

FIGURE 12. Combined visualization for Example 3 ($n = 3$, $T = 1$): L^2 error convergence (left panel) and corresponding EOC values (right panel).

8.5. **Discussion of Numerical Performance.** The numerical experiments validate the proposed Bernoulli–Chebyshev spectral collocation method, demonstrating spectral accuracy with errors decreasing from 10^{-3} to 10^{-12} in agreement with Theorem 7.3. Despite the $O(N^{n+1})$ growth in degrees of freedom, the method scales effectively to three dimensions owing to the sparse structure of the operational matrices and tensor-product bases. Furthermore, the scheme proves robust against multi-harmonic forcing terms and achieves high accuracy ($< 10^{-10}$) with moderate polynomial degrees ($N \leq 14$), thereby avoiding the stringent time-step restrictions typical of explicit finite-difference schemes.

All computations were performed in Python 3.10 using Google Colab with standard runtime resources (Intel Xeon CPU, 13 GB RAM). Numerical linear algebra operations were handled via `NumPy` and `SciPy` (v1.11+), with sparse linear systems solved using `scipy.sparse.linalg.spsolve` (which interfaces with UMFPACK/SuperLU backends). Typical solution times ranged from approximately 0.3 s (1-D, $N = 14$) to 58 s (3-D, $N = 14$), depending on runtime allocation and problem dimensionality.

9. Conclusion

In this research, the Cauchy–Dirichlet problem for an n-dimensional non-homogeneous hyperbolic equation with a p-th degree multi-harmonic trigonometric source term has been completely solved analytically and numerically. By applying the method of eigenfunction expansion and the Binomial Theorem, we achieved the representation of the general solution as an n-fold Fourier series, establishing existence and uniqueness in Sobolev spaces $H_0^1(\Omega) \times L^2(\Omega)$ with proven convergence in the energy norm. Complementing this, we developed a Bernoulli–Chebyshev spectral collocation method using operational matrices and tensor-product structures, which demonstrates exponential convergence and computational efficiency while bypassing stability constraints like the CFL condition. These results provide a rigorous theoretical foundation and a robust numerical benchmark for analyzing complex wave propagation and resonance phenomena in higher-dimensional spaces.

Conflicts of Interest: The authors declare that there are no conflicts of interest regarding the publication of this paper.

References

[1] Z.D. Abbasov, D.A. Juraev, O.K. Abdullaev, I. Nurhidayat, M.A. Shah, Heat Transfer in n-Dimensional Parallelepipeds under Zero Dirichlet Conditions, Eng. Rep. 7 (2025), e70458. https://doi.org/10.1002/eng2.70458.

[2] Z.D. Abbasov, Y.H. Youssri, Fibonacci Collocation Spectral Method and Error Analysis for Heat Conduction Waves in an n-Dimensional Domain, Open J. Math. Sci. 10 (2026), 341–364. https://doi.org/10.30538/oms2026.0291.

[3] Z.D. Abbasov, G. Albeladi, M. Gamal, Y.H. Youssri, Analytical and Numerical Analysis of Multidimensional Diffusion Processes in L^2 Space under Third-Kind Boundary Conditions, Axioms 15 (2026), 380. https://doi.org/10.3390/axioms15050380.

[4] N.S. Koshlyakov, Fundamentals of Differential Equations of Mathematical Physics, Fizmatgiz, 1962.

[5] A.N. Tikhonov, A.A. Samarskii, Equations of Mathematical Physics, Nauka, 1972.

[6] S.L. Sobolev, Equations of Mathematical Physics, Nauka, 2009.

[7] O.A. Ladyzhenskaya, The Boundary Value Problems of Mathematical Physics, Springer, 1985.

[8] V.P. Mikhailov, Partial Differential Equations, Nauka, 1999.

[9] D.H. Sattinger, On Global Solution of Nonlinear Hyperbolic Equations, Arch. Ration. Mech. Anal. 30 (1968), 148–172. https://doi.org/10.1007/BF00250942.

[10] Z.D. Abbasov, Mathematical Physics Equations, Baku, 2018.

[11] Z.D. Abbasov, Partial Differential Equations, Textbook, Ganja, Azerbaijan, 2024.

[12] I.M. Askerov, On a Determination of the Boundary Function in the Initial-Boundary Value Problem for the Second Order Hyperbolic Equation, J. Contemp. Appl. Math. 12 (2022), 45–50.

[13] C. Canuto, M.Y. Hussaini, A. Quarteroni, T.A. Zang, Spectral Methods: Fundamentals in Single Domains, Scientific Computation, Springer Berlin Heidelberg, 2006. https://doi.org/10.1007/978-3-540-30726-6.

[14] J. Shen, T. Tang, L.-L. Wang, Spectral Methods: Algorithms, Analysis and Applications, Springer Series in Computational Mathematics, vol. 41, Springer Berlin Heidelberg, 2011. https://doi.org/10.1007/978-3-540-71041-7.

[15] E.H. Doha, Y.H. Youssri, M.A. Zaky, Spectral Solutions for Differential and Integral Equations with Varying Coefficients Using Classical Orthogonal Polynomials, Bull. Iran. Math. Soc. 45 (2019), 527–555. https://doi.org/10.1007/s41980-018-0147-1.

[16] M.S. Touati Brahim, Y.H. Youssri, A. Alburaikan, H. Khalifa, T. Radwan, R. Hafez, A Refined Galerkin Approach for Solving Higher-Order Differential Equations via Bernoulli Polynomials, Fractals 33 (2025), 2540183. https://doi.org/10.1142/S0218348X25401838.

[17] R.M. Hafez, M.A. Abdelkawy, Y.H. Youssri, A. Biswas, Spectral Bernoulli–Gauss Collocation Scheme for Pantograph-Type Volterra Integro-Differential Equations, Contemp. Math. 7 (2026), 1553–1571. https://doi.org/10.37256/cm.7220268911.

[18] M. Abdelhakem, D. Abdelhamied, M. El-Kady, Y.H. Youssri, Enhanced Shifted Tchebyshev Operational Matrix of Derivatives: Two Spectral Algorithms for Solving Even-Order BVPs, J. Appl. Math. Comput. 69 (2023), 3893–3909. https://doi.org/10.1007/s12190-023-01905-4.

[19] M. Abdelhakem, D. Abdelhamied, M. El-Kady, Y.H. Youssri, Two Modified Shifted Chebyshev–Galerkin Operational Matrix Methods for Even-Order Partial Boundary Value Problems, Bound. Value Probl. 2025 (2025), 34. https://doi.org/10.1186/s13661-025-02021-x.

[20] W.M. Abd-Elhameed, Y.H. Youssri, New Formulas of the High-Order Derivatives of Fifth-Kind Chebyshev Polynomials: Spectral Solution of the Convection–Diffusion Equation, Numer. Methods Partial Differ. Equ. 40 (2024), e22756. https://doi.org/10.1002/num.22756.

[21] Y.H. Youssri, A.G. Atta, Explicit Chebyshev Collocation Method for Multi-Order Fractional Nonlinear Boundary Value Problems in Mathematical Chemistry, Iran. J. Math. Chem. 16 (2025), 257–273. https://doi.org/10.22052/ijmc.2025.256602.1997.

[22] E.H. Doha, R.M. Hafez, Y.H. Youssri, Shifted Jacobi Spectral-Galerkin Method for Solving Hyperbolic Partial Differential Equations, Comput. Math. Appl. 78 (2019), 889–904. https://doi.org/10.1016/j.camwa.2019.03.011.

[23] P. Agarwal, Z.D. Abbasov, S. Jain, F. Tank, Correct Solution of the Mixed Boundary Value Problem for the n-Dimensional Wave Equation, Discret. Contin. Dyn. Syst. Ser. S (2026). https://doi.org/10.3934/dcdss.2026171.

[24] R. Tremblay, S. Gaboury, B.-J. Fugère, A New Class of Generalized Apostol–Bernoulli Polynomials and Some Analogues of the Srivastava–Pintér Addition Theorem, Appl. Math. Lett. 24 (2011), 1888–1893. https://doi.org/10.1016/j.aml.2011.05.012.